Extreme ultraviolet supercontinua supporting pulse durations of less than one atomic unit of time

Hiroki Mashiko, Steve Gilbertson, Michael Chini, Ximao Feng, Chenxia Yun, He Wang, Sabih D. Khan, Shouyuan Chen, and Zenghu Chang*

J. R. Macdonald Laboratory, Department of Physics, Kansas State University, Manhattan, Kansas 66506, USA
**Corresponding author: chang@phys.ksu.edu*

Received August 6, 2009; accepted September 4, 2009;
posted October 2, 2009 (Doc. ID 115348); published October 27, 2009

Double optical gating of high-harmonic generation was used to obtain supercontinuous spectra in the extreme UV (XUV) region including the water window. The spectra supported a 16 as pulse duration that is below one atomic unit of time (24 as). The dependence of the gated spectra on the carrier-envelope phase of the laser provided evidence that isolated attosecond pulses were generated. In addition, to ensure the temporal coherence of the XUV light, the pulse shape and phase of isolated 107 as XUV pulses using a portion of the spectrum were characterized by attosecond streaking. © 2009 Optical Society of America

OCIS codes: 320.7090, 020.2649.

The characteristic time scale for electron motion is the atomic unit of time, which is 24 as. The generation of isolated pulses with such a pulse duration will have a profound impact on the study of electron dynamics. At the present time, the shortest pulses generated are 80 as with 8% satellite pulses, which were generated with linearly polarized 3.6 fs lasers [1]. Even shorter driving lasers are required for generating 24 as pulses with this approach, which is extremely challenging considering that the laser is already close to the one-optical-cycle limit of 2.5 fs for Ti:sapphire lasers. Another method to produce supercontinuous spectra is polarization gating; 130 as pulses were generated from 5 fs lasers [2]. However, because of depletion of the ground state population of the target gas by the circularly polarized leading edge, polarization gating also required short driving laser pulses [3].

A spectrum with 75 eV FWHM is needed to support a 24 as Gaussian pulse. Thus, the harmonics cutoff should be extended to the short-wavelength region. More than ten years ago, harmonics had already reached the water window region between 2 and 4 nm [4,5]. However, in those cases, the spectra corresponded to attosecond pulse trains. Previously, the double optical gating (DOG) technique for generating isolated attosecond pulses with multicycle lasers was demonstrated, combining polarization gating and two-color gating [6,7]. The advantage is reduced depletion of the ground state population by the leading edge of the field [8]. Here, to generate pulses shorter than one atomic unit of time, DOG was implemented with a higher driving laser intensity to extend the width of the extreme UV (XUV) continuum spectra.

A Ti:sapphire amplifier followed by a hollow-core fiber compressor produced 8 fs, 0.8 mJ pulses centered at 790 nm at 1 kHz with carrier-envelope (CE) phase stabilization [9]. The DOG was constructed by two birefringent quartz plates and a BBO (β-BaB_2O_4)crystal [10]. The first quartz plate had a thickness of 270 μm. The second quartz plate and the BBO had thicknesses of 440 and 140 μm, respectively. The estimated polarization gate width is ~2.5 fs, equal to nearly one optical cycle. The estimated pulse duration of the second-harmonic pulse was 20 fs with an energy of 80 μJ [11]. A spherical mirror with a 125 mm focal length was used to focus the laser beam onto a cell filled with neon gas with backing pressure of 600 hPa. The cell was a glass tube with inner diameter of 1.4 mm. The spot sizes of the IR and the second-harmonic beams were 10 and 8 μm, respectively. The estimated peak intensity with DOG was 1.4×10^{16} W/cm^2 at the focal point. The gas cell was located ~1 mm after the focal point for phase matching.

The generated XUV beam passed through a 500 μm hole located 200 mm after the gas cell to reduce the fundamental beam because of its larger divergence angle as compared with the XUV beam. The spectra were dispersed with two types of transmission grating with different groove densities [12]. The 2000 lines/mm grating can observe wavelengths from 15 to 45 nm with a diffraction efficiency of nearly 4% and resolution of 0.013 nm at 15 nm. The 5000 lines/mm grating corresponded to wavelengths below 15 nm with an efficiency of nearly 1.5%. The resolution is 0.05 nm at 2 nm. The spectral images were captured by a microchannel plate imaging detector with a phosphor screen and a cooled CCD camera.

Figure 1(a) shows the high-order harmonic spectra from DOG and linearly polarized pulses. The spectra above and below 15 nm were measured with the 2000 and 5000 lines/mm gratings, respectively. The acceptance angle of the spectrometer was smaller than the beam divergence angle in the vertical direction, thereby clipping the spectrum. To obtain good statistics, spectra from 100,000 laser shots were integrated for each image. Figure 1(b) shows the spatially integrated spectra. The spectrometer measurement cannot directly indicate whether the continuum spectrum below 8 nm was due to the limited spectral resolution. However, because the harmonic yield depends more strongly on the ellipticity of the laser for the higher harmonic orders, the polarization gate

0146-9592/09/213337-3/$15.00

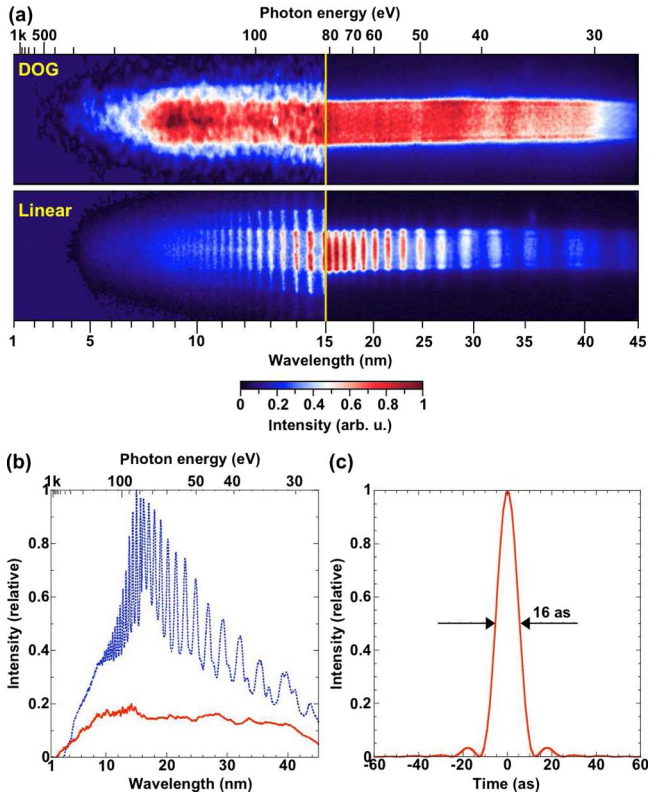

Fig. 1. (Color online) High-harmonic spectra from DOG and linearly polarized pulses. (a) Spectral images from (top) the gated and (bottom) linearly polarized pulses. The yellow vertical line indicates the border between the short- and the long-wavelength regions measured with different gratings. (b) Integrated line spectra from the gated (solid) and linearly polarized (dotted) pulses. (c) Fourier-transform-limited pulses with the gated spectra, assuming flat phase.

width is reduced as the order increases. Thus it is reasonable to believe that the spectrum near the cutoff is continuous when the lower-order plateau harmonics also merged to a continuum as a result of the gating. The entire bandwidth is 2–45 nm (28–620 eV with ~170 eV FWHM). Figure 1(c) shows the Fourier-transform-limited pulse corresponding to the continuous spectrum assuming flat phase. The spectrum supports isolated 16 as pulses, which is below one atomic unit of time.

To ensure that the signal near the cutoff is from XUV light, a boron filter with thickness of 200 nm was placed between the source and the spectrometer. The spectrographs taken with and without the filter are shown in Figs. 2(a) and 2(b), respectively. The line spectra are shown in Fig. 2(c). The sharp absorption edge at 6.6 nm of boron can be clearly seen [13], which serves as wavelength calibration while also confirming that the signal was indeed from XUV, not scattered laser light. The cutoff was 2 nm, which is well within the water window.

The spectrum intensity changes periodically with the CE phase as shown in Fig. 3. The 2π periodicity is evidence of DOG [6]. This is caused by the shift of the driving laser field inside the polarization gate as the CE phase is varied [8]. The results indicate that DOG works for the entire spectral region, which is

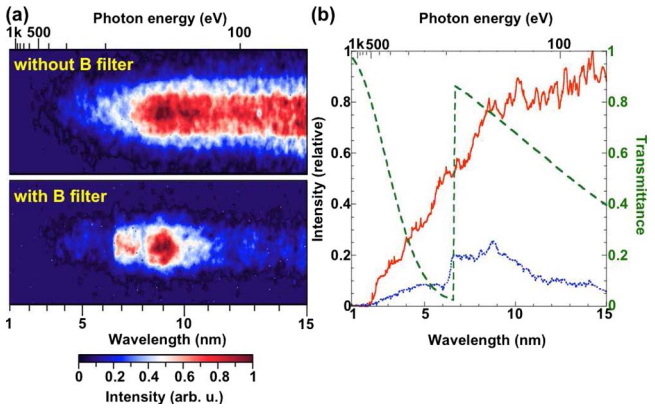

Fig. 2. (Color online) High-harmonic spectra in the short-wavelength region. (a) Harmonic spectral images (top) without and (bottom) with the boron filter. (b) Integrated line spectra with (dotted) and without (solid) the boron filter. The filter transmittance is given by the green dashed curve.

evidence of the single-cycle gate width, while the spectra support isolated attosecond pulses including the water window range.

To ensure the temporal coherence of the harmonics, we used the method of complete reconstruction of attosecond bursts (CRAB) based an attosecond streaking [7,14]. The optical configuration is described in [15]. The XUV beam generated in neon gas passed through an aluminum filter (300 nm thickness). The XUV beam was focused by a Mo/Si mirror with a reflection bandwidth of 19–35 nm and reflectivity of ~8% [16]. An annular silver coated mirror was used to focus the streaking IR beam. A neon-gas-filled jet was placed at the beam focus. The photoelectrons were measured by a time-of-flight spectrometer.

Figures 4(a) and 4(b) show the measured and the reconstructed CRAB traces, respectively. The attosec-

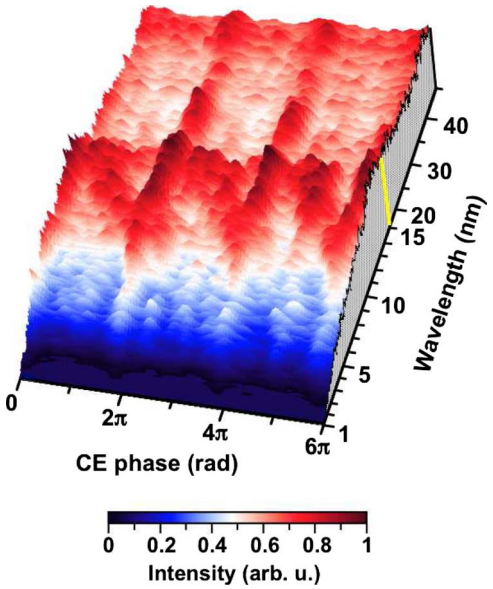

Fig. 3. (Color online) CE phase dependence of the XUV spectrum generated with DOG. The yellow vertical line indicates the border between the short- and the long-wavelength regions measured with different gratings.

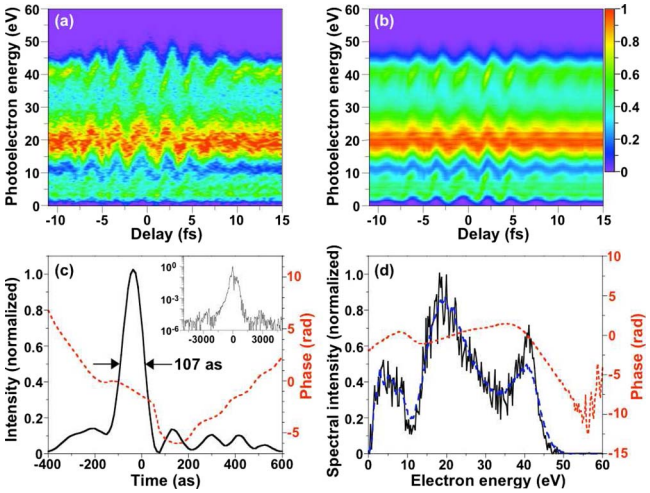

Fig. 4. (Color online) Measurement of the isolated attosecond pulse with CRAB. (a) Measured CRAB trace. (b) Reconstructed CRAB trace. (c) Reconstructed XUV pulse shape (solid curve) and phase (dotted curve). (d) Reconstructed XUV spectrum (solid) and phase (dotted). Also shown is the measured XUV spectrum (dashed curve) without the streaking laser for marginal comparison.

ond pulse was reconstructed by using a blind iterative algorithm, PCGPA [17]. The reconstructed temporal profile and phase show a 107 as pulse duration as shown in Fig. 4(c). The prepulses and postpulses are suppressed to less than a 1% contribution. In addition, the measured and the reconstructed harmonic spectra agree well, as shown in Fig. 4(d). At this time the pulse duration was limited by the bandwidth of the Mo/Si mirror and the residual pulse dispersion. However, although only a portion of the spectrum was used, the coherence of the harmonics was not destroyed. Thus, isolated attosecond pulses in the water window region could be generated.

In conclusion, we generated XUV supercontinuous spectrum with a bandwidth from 2 to 45 nm (28–620 eV) by implementing DOG. The spectra are capable of supporting 16 as pulses, which are shorter than one atomic unit of time. Of course, many issues will have to be resolved, such as compensating the chirp [18]. The CE phase dependence of the spectra including the water window range with 2π periodicity was observed for the first time (to our knowledge), which indicates that DOG works for the entire spectral region and supports single attosecond pulses. In addition, the measurement of the isolated 107 as pulse confirms the coherence of the XUV light. The pulses covering the water window may also be used to image live biological samples with a time resolution much higher than the synchrotron sources.

H. Mashiko and S. Gilbertson contributed equally to this work. This material is supported by the U.S. Army Research Office under grant W911NF-07-1-0475, the National Science Foundation (NSF) under grant 0457269, and by the U.S. Department of Energy (DOE).

References

1. E. Goulielmakis, M. Schultze, M. Hofstetter, V. S. Yakovlev, J. Gagnon, M. Uiberacker, A. L. Aquila, E. M. Gullikson, D. T. Attwood, R. Kienberger, F. Krausz, and U. Kleineberg, Science **320**, 1614 (2008).
2. G. Sansone, E. Benedetti, F. Calegari, C. Vozzi, L. Avaldi, R. Flammini, L. Poletto, P. Villoresi, C. Altucci, R. Velotta, S. Stagira, S. De. Silvestri, and M. Nisoli, Science **314**, 443 (2006).
3. Z. Chang, Phys. Rev. A **70**, 043802 (2004).
4. Ch. Spielmann, N. H. Burnett, S. Santania, R. Koppitsch, M. Schnürer, C. Kan, M. Lenzner, P. Wobrauschek, and F. Krausz, Science **278**, 661 (1997).
5. Z. Chang, A. Rundquist, H. Wang, M. M. Murnane, and H. C. Kapteyn, Phys. Rev. Lett. **79**, 2967 (1997).
6. H. Mashiko, S. Gilbertson, C. Li, S. D. Khan, M. M. Shakya, E. Moon, and Z. Chang, Phys. Rev. Lett. **100**, 103906 (2008).
7. H. Wang, M. Chini, S. D. Khan, S. Chen, S. Gilbertson, X. Feng, H. Mashiko, and Z. Chang, J. Phys. B **42**, 134007 (2009).
8. Z. Chang, Phys. Rev. A **76**, 051403(R) (2007).
9. H. Mashiko, C. M. Nakamura, C. Li, E. Moon, H. Wang, J. Tackett, and Z. Chang, Appl. Phys. Lett. **90**, 161114 (2007).
10. S. Gilbertson, H. Mashiko, C. Li, S. D. Khan, M. M. Shakya, E. Moon, and Z. Chang, Appl. Phys. Lett. **92**, 071109 (2008).
11. SNLO software, http://www.as-photonics.com/SNLO.html.
12. B. Shan and Z. Chang, Phys. Rev. A **65**, 011804(R) (2002).
13. B. L. Henke, E. M. Gullikson, and J. C. Davis, At. Data Nucl. Data Tables **54**, 181 (1993).
14. Y. Mairesse and F. Quéré, Phys. Rev. A **71**, 011401(R) (2005).
15. S. Gilbertson, X. Feng, S. D. Khan, M. Chini, H. Wang, H. Mashiko, and Z. Chang, Opt. Lett. **34**, 2390 (2009).
16. M. Hatayama, H. Takenaka, E. M. Gullikson, A. Suda, and K. Midorikawa, Appl. Opt. **48**, 5464 (2009).
17. M. Chini, H. Wang, S. D. Khan, S. Chen, and Z. Chang, Appl. Phys. Lett. **94**, 161112 (2009).
18. Z. Chang, Phys. Rev. A **71**, 023813 (2005).